RAPID COMMUNICATION

Transport coefficients and mechanical response in hard-disk colloidal suspensions*

Bo-Kai Zhang(张博凯)[1,†], Jian Li(李健)[3], Kang Chen(陈康)[2], Wen-De Tian(田文得)[2], and Yu-Qiang Ma(马余强)[1,2]

[1] National Laboratory of Solid State Microstructures and Department of Physics, Nanjing University, Nanjing 210093, China
[2] Center for Soft Condensed Matter Physics & Interdisciplinary Research, College of Physics, Optoelectronics and Energy, Soochow University, Suzhou 215006, China
[3] Department of Physics, Nanjing Normal University, Nanjing 210023, China

(Received 14 June 2016; revised manuscript received 22 July 2016; published online 30 September 2016)

We investigate the transport properties and mechanical response of glassy hard disks using nonlinear Langevin equation theory. We derive expressions for the elastic shear modulus and viscosity in two dimensions on the basis of thermal-activated barrier-hopping dynamics and mechanically accelerated motion. Dense hard disks exhibit phenomena such as softening elasticity, shear-thinning of viscosity, and yielding upon deformation, which are qualitatively similar to dense hard-sphere colloidal suspensions in three dimensions. These phenomena can be ascribed to stress-induced "landscape tilting". Quantitative comparisons of these phenomena between hard disks and hard spheres are presented. Interestingly, we find that the density dependence of yield stress in hard disks is much more significant than in hard spheres. Our work provides a foundation for further generalizing the nonlinear Langevin equation theory to address slow dynamics and rheological behavior in binary or polydisperse mixtures of hard or soft disks.

Keywords: soft matter, colloidal suspensions, glass transition, rheology

PACS: 61.43.Fs, 64.70.kj, 64.70.pv **DOI:** 10.1088/1674-1056/25/11/116101

1. Introduction

The viscoelasticity of glass is an intriguing subject in rheology and condensed matter physics, and is of both theoretical and technological importance.[1,2] Developing microscopic predictive theory for macroscopic rheological properties and mechanical responses remains a major challenge. In crystals, rigidity is attributed to the long-range density correlation.[3] In amorphous materials, the glass transition occurs upon cooling (thermal-driven system) or densification (density-driven system), and is accompanied by the emergence or significant rise of shear elasticity.[4] Such shear resistance cannot be interpreted as the consequence of long-range correlation, as glass lacks long-range order. Instead, it is related to the rigidity of the local cage where the motion of a particle is restricted by its neighbors.[5] The rigidity of the cage, or the barrier for a particle to escape the cage, increases upon cooling or densification, leading to larger shear elasticity. Phenomenological and several microscopic theories have been constructed to predict the rheological and mechanical quantities.[6–12] For instance, the phenomenological "soft glass rheology" (SGR) model is a well-known theoretical approach to predict the transport properties of soft amorphous materials. SGR is based on Bouchaud's trap model, and has been developed to address the impact of strain in mesoscopic elements on the local barrier-hopping process. In the SGR model, the trapped energy is often supposed to have a harmonic form that lacks microscopic interpretation, and hence limits its quantitative and material-specific predictive ability.[6–9] The first-principles microscopic mode-coupling theory (MCT) and dynamic mean field p-spin glass models have been extended to address the shear acceleration of glassy dynamics by de-correlating the memory function that dictates the cage constraint.[10–12] However, the activated hopping process, which dominates the structural relaxation in the deeply supercooled regime, is missing in these theories.

Recently, considerable attention has been paid to two-dimensional (2D) colloidal glass. The 2D colloidal assembly can be realized experimentally by, for example, confining colloidal particles at the water–air interface.[13–16] An approach based on the positional data of 2D colloids recorded by video microscope and simulations of hard disks has been developed to determine the shear modulus and elastic dispersion relations for 2D colloidal glass.[16] The glass transition and elasticity of hard disks has also been studied by MCT.[17] The localization lengths at the transition are similar in 2D and 3D colloids, correlating to the Lindemann melting criterion. Fuchs and coworkers have studied the elasticity of binary mixed 2D hard disks, and found that mixing different components causes the softening of the elastic modulus.[18,19]

Based on structural information about the materials, the microscopic nonlinear Langevin equation (NLE) theory for supercooled liquid and glass can capture the physics of lo-

*Project supported by the National Basic Research Program of China (Grant No. 2012CB821500) and the National Natural Science Foundation of China (Grant Nos. 21374073 and 21574096).

†Corresponding author. E-mail: bkzhang@smail.nju.edu.cn

© 2016 Chinese Physical Society and IOP Publishing Ltd

cal caging and activated barrier-hopping dynamics.[20–25] The NLE theory has already been successfully applied to the slow dynamics and mechanical response of hard-sphere colloidal glass and polymer glasses.[5,20,26–29] In previous work, we extended NLE theory to quiescent 2D hard disks.[30] Here, we further extend the theory to address the transport properties and mechanical response of glassy hard disks. On the basis of the Green–Kubo linear response theory[31] and the modified binary collision mean field (BCMF) theory,[32,33] the elastic shear modulus and viscosity can be formulated in terms of the static structure, dynamic localization length, and hopping time. The external load affects the viscoelastic properties by effectively altering the dynamic localization length and barrier, i.e., distorting the dynamic free energy or "the dynamic free e". Quantitative comparisons of the dynamic characteristic length scales, barrier, transport coefficients, and relevant mechanical control variable relations between 2D and 3D colloidal suspensions are presented. The data for 3D hard-sphere colloids are taken from or obtained following the approach of Schweizer.[28]

The remainder of this paper is organized as follows. In Section 2, we recall the basics of NLE theory for hard disks and introduce its generalization to include mechanical deformation. Section 3 describes the elastic shear modulus, viscosity, and alteration of the profile of dynamical free energy under mechanical deformation and the stress–strain relation. We conclude in Section 4.

2. Nonlinear Langevin equation theory

2.1. Basics

NLE theory describes the localized–delocalized motion of a "tagged" particle through the stochastic equation for the scalar displacement $r(t)$ of the particle[30]

$$\zeta_{\rm s}\frac{\partial r(t)}{\partial t} = -\frac{\partial F_{\rm eff}[r(t)]}{\partial r(t)} + \delta f(t), \tag{1}$$

where $\zeta_{\rm s}$ is a short-time friction constant and the white noise fluctuating force satisfies $\langle \delta f(0)\delta f(t)\rangle = 4\beta^{-1}\zeta_{\rm s}\delta(t)$. The crucial quantity in Eq. (1) is the "dynamic free energy" $F_{\rm eff}$, which dictates the effective many-body interaction on the tagged particle by the surrounding particles. The term $-\partial F_{\rm eff}(r)/\partial r$ can be regarded as the effective restoring force of the cage. The dynamic free energy for hard disks is given by[30]

$$\beta F_{\rm eff}(r) = -2\ln(r) - \int \frac{{\rm d}q}{(2\pi)^2}\rho C^2(q)S(q)\left[1+S^{-1}(q)\right]^{-1} \times \exp\left\{-\frac{q^2r^2}{4}\left[1+S^{-1}(q)\right]\right\}, \tag{2}$$

where β is the inverse of the temperature. $C(q)$ and $S(q)$denote the direct correlation function and static structure factor, respectively.[34] $C^2(q)S(q)$ quantifies the effect of the cage structure, and ρ is the number density of particles. In density functional theory (DFT),[35] $F_{\rm eff}(r)$ describes the competition between localized (nonzero r) and delocalized states ($r=\infty$). The leading "ideal" entropic-like term favors the fluid state, and the second "interaction" term corresponds to an entropic trapping potential favoring localization. In the supercooled or glass state, the theory predicts a barrier in the profile of $F_{\rm eff}(r)$, indicating that the particle is localized in a cage after a short time and escapes through an activated hopping process. Throughout this paper, we adopt the Guo–Riebel method to obtain the static structures of 2D colloidal suspensions.[30,36] A barrier emerges at $\phi > \phi_{\rm c} = 0.612$, where $\phi_{\rm c}$ is the crossover packing fraction. Some characteristic lengths are marked in the inset of Fig. 1. The localization length $r_{\rm LOC}$ and barrier length $r_{\rm B}$ denote the positions of the local minimum and maximum (nonzero) of the profile of $F_{\rm eff}(r)$. R^* corresponds to the location of the maximum restoring force. In a deeply supercooled regime, activated hopping events dominate the relaxation process, and so the mean barrier-hopping time τ_α is expected to be close to the relaxation time α. Based on the overdamped version of Kramers' first-passage theory,[37] this relaxation time yields

$$\frac{\tau_\alpha}{\tau_0} = \frac{2\pi g(\sigma)}{\sqrt{K_0 K_{\rm B}}}{\rm e}^{F_{\rm B}/k_{\rm B}T}, \tag{3}$$

where τ_0 is the elementary Brownian diffusion time, σ is the particle diameter, and $g(\sigma)$ is the contact value of the radial distribution function. K_0 and $K_{\rm B}$ are the curvatures of the local minimum and barrier, respectively. $F_{\rm B}$ is the barrier height, which is the main factor in determining the hopping time under the deeply supercooled or glass state.

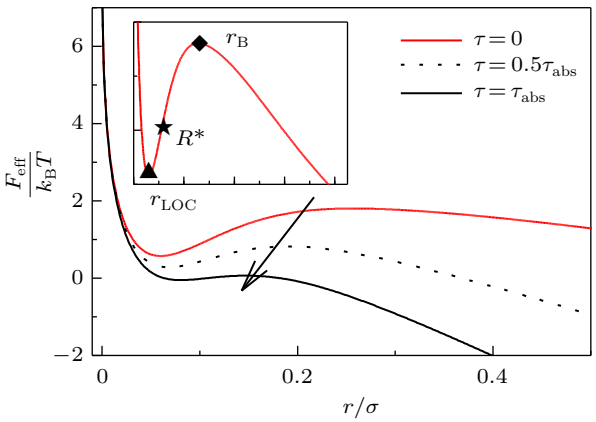


Fig. 1. (color online) Dynamic free energy as a function of scalar displacement r at volume fraction $\phi = 0.709$ for three typical shear stresses. The three characteristic lengths are marked in the inset.

2.2. Elastic shear modulus and viscosity

The elastic shear modulus for hard disks follows the standard Green–Kubo formula[19]

$$G' = \beta\rho\sum_{ij}^{N}\langle\tau_i(t\to\infty)\tau_j(0)\rangle$$

$$= \frac{k_B T}{32\pi\sigma}\int_0^\infty \mathrm{d}qq^3\left[\frac{\mathrm{d}}{\mathrm{d}q}\ln(S(q))\right]^2 \times \exp\left(-q^2 r_{\mathrm{LOC}}^2/2S(q)\right), \quad (4)$$

where $\tau_i(t) = f_i x_i$ is the microscopic shear stress. The final expression on the right-hand side is the native version of the MCT shear modulus. Similarly, the shear viscosity is expressed as the time integral of the collective stress time correlation function

$$\eta(\phi,\omega) = \eta_\infty(\phi) + \frac{\beta}{V}\sum_{ij}\int_0^\infty \langle\tau_i(t)\tau_j(0)\rangle\, \mathrm{e}^{\mathrm{i}\omega t}\,\mathrm{d}t.$$

Following the procedure in Refs. [27] and [29], we have

$$\eta(\phi) = \eta_\infty(\phi) + \frac{k_B T}{64\pi\sigma}\int_0^\infty \mathrm{d}qq\left(\frac{\partial}{\partial q}\ln S(q)\right)^2 \frac{1}{D_S^C(q)}, \quad (5)$$

where $\eta_\infty(\phi) = \eta_0 g(\sigma)$ is the high-frequency viscosity. D_S^C is the collective diffusion coefficient that is determined by a generalization of BCMF theory, including an activated barrier hopping contribution to the friction constant[32]

$$D_S^C(q) = \frac{D_0}{S(q)[g(\sigma)d(q)^{-1} + \zeta_{\mathrm{hop}}/\zeta_s]}, \quad (6)$$

$$\zeta_{\mathrm{HOP}} = k_B T/D_{\mathrm{HOP}} = 4\zeta_0\frac{\tau_\alpha}{\tau_0}L_D^{-2}, \quad (7)$$

$$d(q) = [1 - j_0(q\sigma) + 2j_2(q\sigma)]^{-1}. \quad (8)$$

D_0 is the diffusion constant of solvent, $d(q)$ quantifies the two-particle collisions on a length scale $2\pi/q$, and j_i is the i-th Bessel function. ζ_s is the short-time friction constant and ζ_{HOP} is the modified friction coefficient including the activated hopping contribution. The modified friction coefficient dominates the single-particle diffusion beyond the supercooled regime ($\phi > \phi_c$). The length $L_D \sim 0.78\sigma$ describes the mean diffusive jump distance, independent of the volume fraction.

2.3. Theory for mechanical deformation

When a load is applied, strain softening of the modulus and shear thinning of the viscosity occur. Microscopically, in the spirit of the trap model, the stress deforms the local cage, and the motion of particles is accelerated directionally to release this deformation. Based on such a physical picture, the accelerated hopping dynamics of particles are mimicked in a modified dynamic free energy by introducing a type of mechanical work contribution, $F(r) = F(r;\tau=0) - f_{\mathrm{micro}}r$.[27] This idea is analogous to the Eyring model[38] in which, however, the work-like term is added directly to the barrier.[24] The quantitative connection between macroscopic stress τ and microscopic force f_{micro} is not straightforward. In the spirit of an "isotropically sheared hard sphere model",[12] it can be assumed that the external shear stress propagates into the interior of the material and is distributed uniformly across the particles, i.e., the microscopic force equals the macroscopic stress acting on a unit cross-section of the particle.[27] In 2D, we have $f_{\mathrm{micro}} = \tau_{\mathrm{macro}}\langle A\rangle/\phi^{1/2}$. The cross-sectional area can be approximated as $\langle A\rangle = \phi^{1/2}\sigma/\rho^{1/2}$, and hence the microscopic force $f_{\mathrm{micro}} = \lambda\tau/\phi^{1/2}$. We set the uncertain parameter $\lambda = 1$ for simplicity. The expression for the dynamic free energy under shear stress τ is then

$$F(r) = -2\ln(r) - \int\frac{\mathrm{d}q}{(2\pi)^2}\rho C^2(q)S(q)\times\left[1+S^{-1}(q)\right]^{-1} \times\exp\left[q^2/4\alpha[1+S^{-1}(q)]\right] - \frac{\tau}{\phi^{1/2}}r. \quad (9)$$

3. Results

To investigate the distortion of the dynamic free energy under different mechanical variables, we introduce the simplified nonlinear stress–strain relation $\gamma = \tau/G(\tau)$, where γ is the dimensionless strain and $G(\tau)$ can be computed from Eq. (4). Figure 1 shows profiles of the dynamic free energy under stress (Eq. (9)). The influence of stress on the dynamic free energy reduces the barrier, shifts the localization lengths, and alters the well and barrier curvatures. The barrier is totally destroyed when the stress reaches a value known as the absolute yield stress τ_{abs}, i.e., under this stress, the glass is mechanically devitrified and the particles flow without any

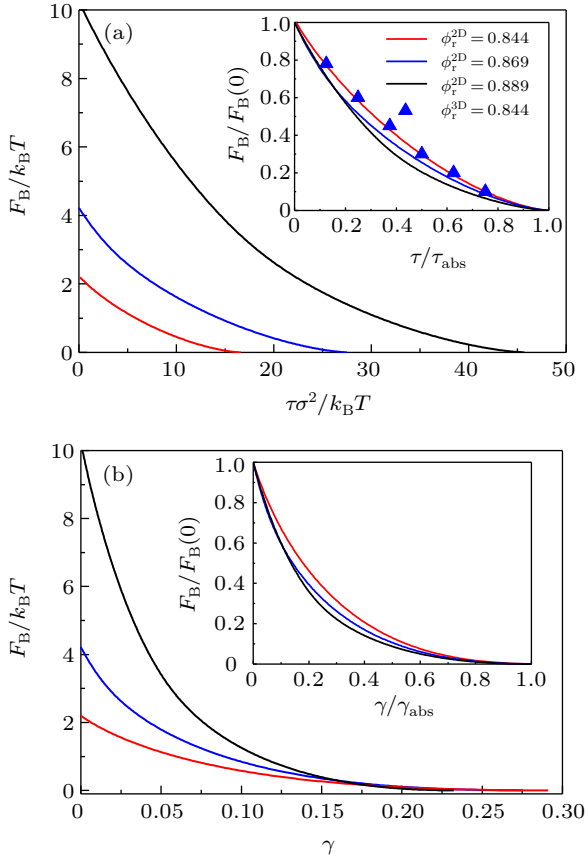


Fig. 2. (color online) (a) Activated barrier as a function of shear stress (in units of k_BT/σ^2) at three volume fractions. The inset shows the same results over a reduced scale. (b) Activated barrier as a function of strain. The inset shows the same results over a reduced scale.

hopping process. Correspondingly, we can define the absolute yield strain $\gamma_{abs} = \tau_{abs}/G(\tau_{abs})$. The dependences of the barrier, localization lengths, and curvatures on the stress or strain are shown in Figs. 2 and 3. The barrier is destroyed when the strain exceeds 20%, which is higher than in the 3D analog. Dimensionless plots of barrier versus stress (inset of Fig. 2(a)) or strain (inset of Fig. 2(b)) show quasi-universal deductions, which are also observed in 3D. r_{loc} (r_b) increases (decreases) with increasing stress or strain (Fig. 3(a)). The curves of r_{loc} and r_b merge at the absolute yield point. Analogous behavior for the well and barrier curvature is apparent in Fig. 3(b). The well curvature controls the vibrational amplitude and frequency of the trapped particle. The vanishing of curvatures corresponds to the localized–delocalized transition of the particle motion.

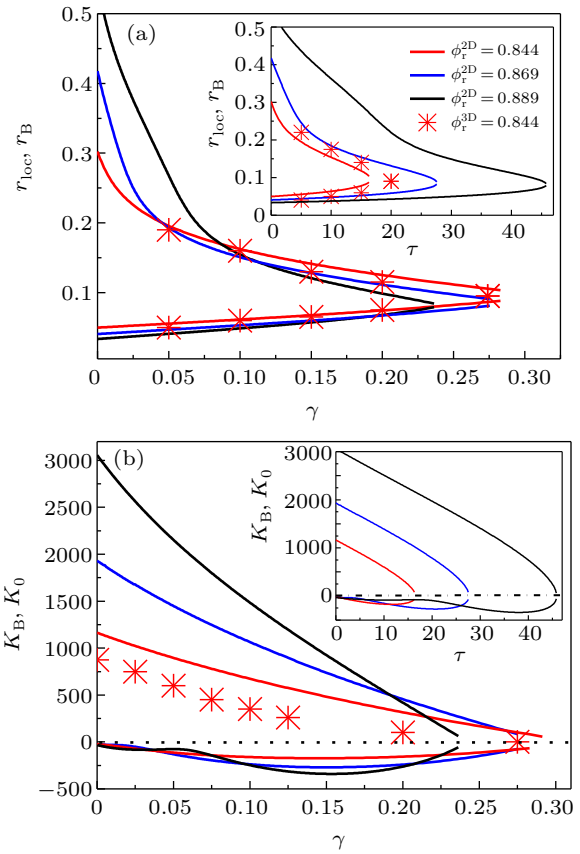


Fig. 3. (color online) (a) Localization length and location of barrier as functions of strain and stress (inset). Data for 3D hard spheres are shown as star symbols for comparison. (b) Well and barrier curvatures as functions of strain and stress (inset). K_0 for 3D hard spheres shown as star symbols.

Figure 4(a) shows the increase in the elastic shear modulus upon densification. The shear modulus increases exponentially $G' = 1.6 \times 10^{-3}\, e^{16.6\phi/\phi_{RCP}} \sim e^{25.9\phi}$ (in units of $k_B T/\sigma^3$) over the entire packing fraction range investigated. As a comparison, the modulus in 3D colloidal suspensions can be fitted by $G' = 4.172 \times 10^{-7}\, e^{23.0\phi/\phi_{RCP}} \sim e^{27.7\phi}$. Plotted versus ϕ/r_{LOC}^2, a roughly linear relationship is obtained at high density. If we use the random close packing fraction ϕ_{RCP} as a normalizing factor, the moduli of 2D and 3D colloidal suspensions are nearly identical at high density. The random close packing fraction for 3D is $\phi_{RCP} = 0.64$, and that for 2D is $\phi_{RCP} = 0.84$. We suggest that $\phi_r = \phi/\phi_{RCP}$ is an appropriate variable for a comparison between different dimensions.[30] The shear viscosity η is related to the elastic shear modulus and the alpha relaxation time. In Maxwell's relation, we have $\eta = G'\tau_\alpha$. Figure 4(b) compares the viscosity obtained from Eq. (5) and Maxwell's relation. The difference in the results is within an order of magnitude over the entire density range investigated. In this range (area fraction from $\phi_r = 0.75$ to $\phi_r = 0.90$), the viscosity of 2D hard disks increases more than seven orders of magnitude; the difference between Eq. (5) and the Maxwell relation is only large at intermediate area fractions and vanishes at low and high densities. The viscosity can be fitted by the exponential form $(\eta/\eta_0)_{2D} = 19.88\, e^{92.39(\phi/\phi_{RCP})^{36.7}}$. We find $(\eta/\eta_0)_{2D} \sim 18$ and $(\eta/\eta_0)_{3D} \sim 10$ at the crossover packing fraction. The kinetic fragility is given by $m_{2D} = 43.8$ and $m_{3D} = 69$ at $\phi/\phi_{RCP} = 0.90625$. When stress is applied, there is a significant decrease in viscosity, as expected (Fig. 4(b)). However, a sharper increase in viscosity (larger fragility) occurs at high density under stress.

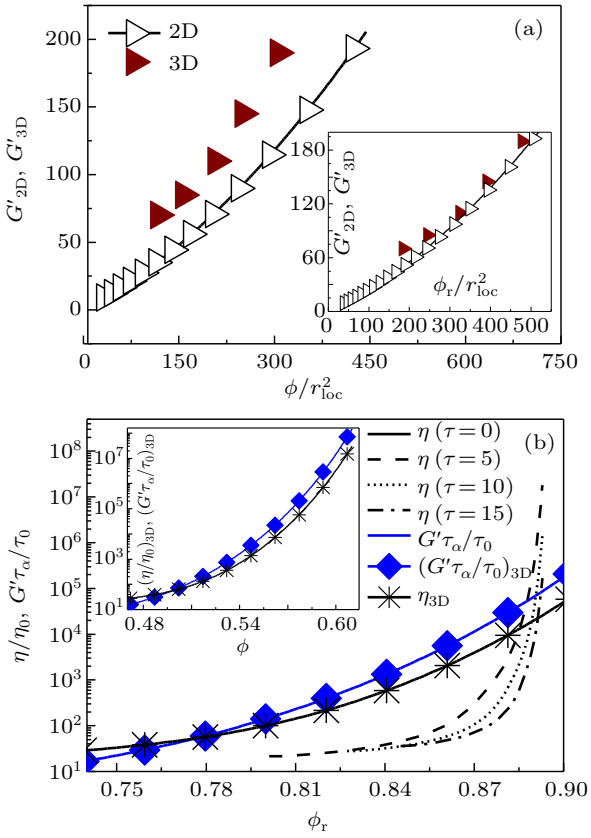


Fig. 4. (color online) Transport coefficients. (a) Quiescent elastic shear modulus as a function of the ratio ϕ/r_{loc}^2 and ϕ_r/r_{loc}^2 (inset), where ϕ_r is the packing fraction reduced by the random close packing fraction ϕ_{RCP}. (b) Shear viscosity and the product of elastic modulus and relaxation time as functions of reduced packing fraction. Data for 3D colloids are shown (line+symbol) for comparison. The viscosity under four different stresses is also shown. The inset shows the viscosity and the product in 3D in a wider range of (normal) packing fraction.

The stress–strain relation is shown in Fig. 5(a). Stress increases with strain until the absolute yielding strain γ_{abs} is reached. The values of γ_{abs} become smaller for denser systems. As in 3D colloids, the absolute yield stress increases exponentially with packing fraction. The dynamic yield stress, which is empirically defined as the stress under which the relaxation time reduces to some value such as $\tau_\alpha/\tau_0 = 10$ or $\tau_\alpha/\tau_0 = 100$, also increases exponentially with the packing fraction at high density (Fig. 5(b)). For $\tau_\alpha/\tau_0 = 100$, τ_y increases more rapidly with the packing fraction. It seems likely that the two curves will merge at sufficiently high area fractions, but our model cannot reach this point. Note that the dynamic yield stress in 2D grows much more rapidly with respect to the packing fraction than in 3D hard spheres. Note also that τ_{dyn} increases from ~ 0.6 to $\tau_{dyn} \approx 10$ when ϕ increases by approximately 1%. For comparison, in 3D hard spheres, ϕ must increase by about 5% to produce the same increment in τ_{dyn}.

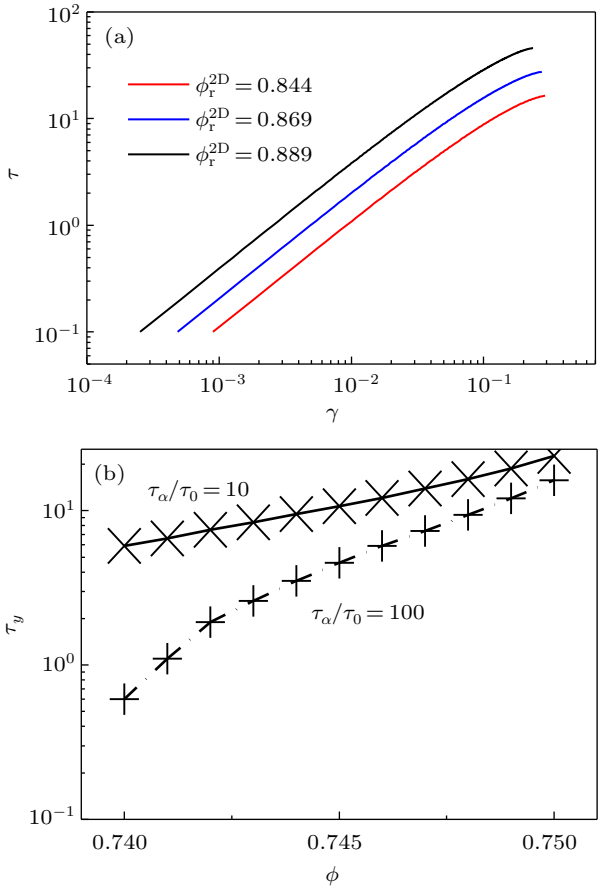


Fig. 5. (color online) (a) Stress–strain relation for packing fractions of $f = 0.844$, 0.869 and 0.889. (b) Dynamic yield stress as a function of packing fraction for relaxation times of $\tau_\alpha/\tau_0 = 10$ and $\tau_\alpha/\tau_0 = 100$.

Figure 6 shows the softening of the elastic shear modulus under deformation. The modulus is normalized by its unperturbed value. The modulus decays faster with stress at lower packing fractions, whereas it decays faster with strain at higher packing fractions. At the same relative packing fraction ϕ_r, the modulus of 2D hard disks decays less rapidly with deformation than that of 3D hard spheres.

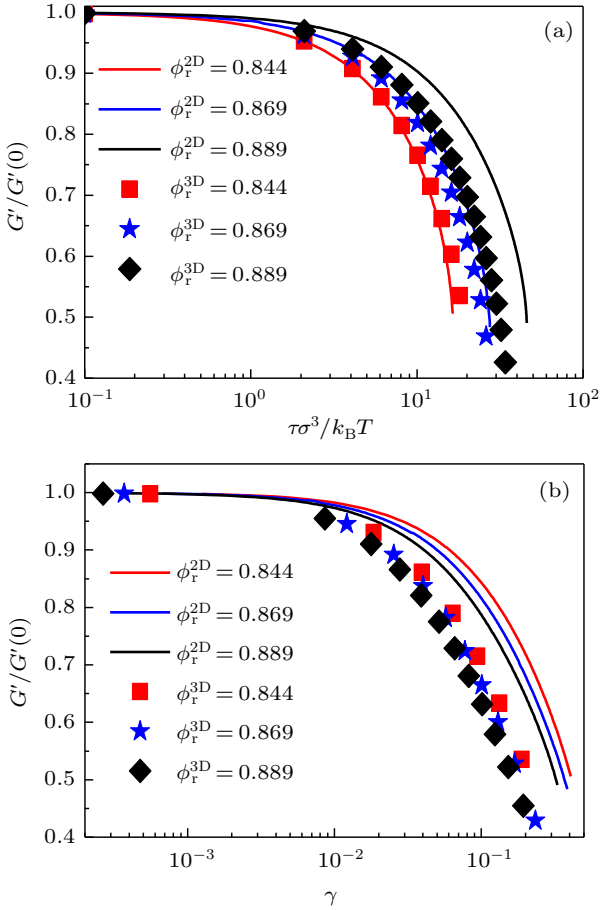


Fig. 6. (color online) Reduced elastic shear modulus as a function of (a) shear stress and (b) strain.

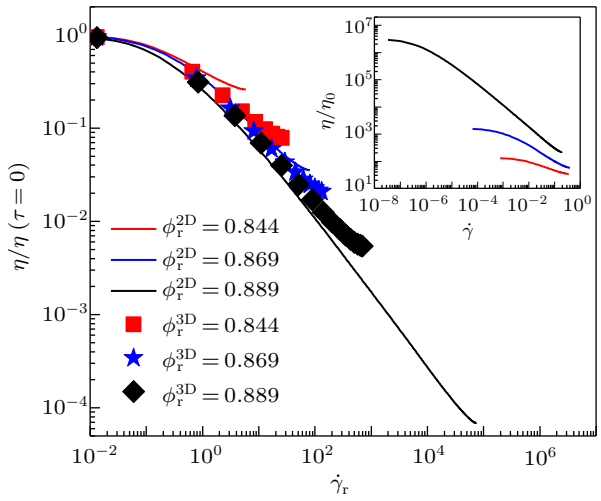


Fig. 7. (color online) Shear viscosity as a function of strain rate. $\dot{\gamma}_r = \dot{\gamma}\tau_{stress}$ is the nondimensionalized strain rate.

In the strain-rate-control deformation, the glass is under plastic flow, which follows the relation $\tau = \dot{\gamma}\eta(\tau)$. One strain rate corresponds to a unique stress and viscosity. Figure 7 shows the typical shear thinning behavior. The reduction of viscosity happens at a smaller strain rate for denser systems (inset of Fig. 7). We nondimensionalize the strain rate using the characteristic stress relaxation time $\tau_{stress} = \eta(\tau = 0)\sigma^3/8k_BT$, i.e., $\dot{\gamma}_r = \dot{\gamma}\tau_{stress}$. The decay in viscosity obeys

a power law $\eta \sim \dot{\gamma}_{\rm r}^{-\Delta}$ at large strain rates. The power-law decay of viscosity spans a larger range of strain rate at higher density. We obtain $\Delta_{\rm 2D} = 0.667$ for 2D hard disks, which is close to the 3D value $\Delta_{\rm 3D} = 0.69$ for $\phi_{\rm r} = 0.889$. This value is consistent with the analytic prediction $\Delta = 2/3$ in the p-spin glass model. The relation between the stress and strain rate is shown in Fig. 8. The flow stress increases monotonically with strain rate. Opposite trends can be observed in the stress for 2D and 3D colloids. At low density, the flow stress of 3D hard spheres is larger than that of 2D hard disks for the same reduced density and strain rate. On the contrary, at high density, the flow stress of 2D hard disks becomes larger.

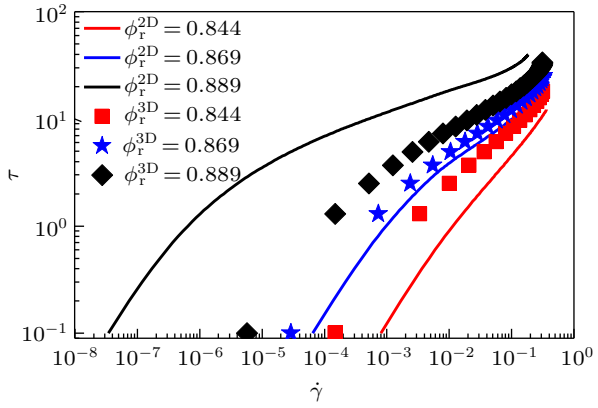


Fig. 8. (color online) Relation between stress and strain rate.

4. Summary and discussion

The nonlinear Langevin equation theory has been extended to study the transport properties and mechanical response of 2D hard disks via the Green–Kubo formula and modified BCMF theory. Expressions for the elastic shear modulus and viscosity of hard disks were derived based on the physical picture of the thermal-activated barrier-hopping dynamics and the mechanically accelerated motion. The dynamic free energy profile is distorted under deformation. The barrier is reduced, and the positions and curvatures of the local well and the barrier shift.

On the basis of the distortion of dynamic free energy, we predict the softening of elasticity and the reduction of shear viscosity under deformation. These phenomena are qualitatively the same as 3D hard spheres. The difference is in the density dependence of viscosity or the product of elastic modulus and relaxation time. Quantitative differences are manifested by comparisons between 2D and 3D colloids based on the same reduced packing fraction. For example, the dynamic yield stress in 2D grows much more rapidly with respect to the packing fraction than in 3D; the flow stress of 2D colloids is smaller (larger) than that of 3D colloids at low (high) density.

In this article, our theory was applied to a spatially homogeneous system in which the mechanical deformation was assumed to be scalar. A static structure factor was supposed to be close to thermal equilibrium because of the slow loading of external force. This work provides a foundation for further generalization of the nonlinear Langevin equation theory to study slow dynamics and rheological behavior in binary or polydisperse mixtures of hard or soft disks and to address the thin film or finite confinement problem.

Appendix A: Derivation of dynamic free energy, shear elastic modulus, and viscosity

Here, we give the full derivation of the dynamic free energy, elastic shear modulus, and viscosity for 2D hard disks using the standard mode-coupling approximation. For more technical details, see Ref. [39]. The dynamic free energy formula for tagged particle in 3D can be derived by two approaches.[21] One is to construct a self-consistent equation for the localization length $r_{\rm LOC}$ based on the native version of mode-coupling theory. The equation gives $F_{\rm eff}$, because the minimum of $F_{\rm eff}(r)$ emerges at the localization length. The second approach determines the equation of motion for the scalar displacement $r(t)$ based on nonequilibrium statistical mechanics. Here, we give the derivation for a 2D system using the first approach. A similar procedure is used to derive the elastic shear modulus and viscosity.

The tagged particle and collective density fluctuations are defined as

$$\rho_{\boldsymbol{q}}^{\rm S} = {\rm e}^{{\rm i}\boldsymbol{q}r^{\rm S}}, \tag{A1}$$

$$\rho_{\boldsymbol{q}} = \sum_{i=1}^{N} ({\rm e}^{{\rm i}\boldsymbol{q}r_i}). \tag{A2}$$

To construct a self-consistent equation for tagged particle displacement, the lowest-order mode-coupling approximation is adopted. The approximation assumes that the bilinear products of density fluctuations, $\rho_{\boldsymbol{q}}\rho_{-\boldsymbol{q}}^{\rm S}$, are only important modes for slow dynamics. The first step towards the derivation starts with the projection of the full evolution operator onto the subspace of the bilinear products

$${\rm e}^{\Omega t} \approx \hat{P}{\rm e}^{\Omega t}\hat{P}, \tag{A3}$$

from which we obtain the projection operator

$$\hat{P} = \sum_{\boldsymbol{q}} \frac{|\rho_{\boldsymbol{q}}\rho_{-\boldsymbol{q}}^{\rm S}\rangle\langle\rho_{-\boldsymbol{q}}\rho_{\boldsymbol{q}}^{\rm S}|}{NS(q)}, \tag{A4}$$

where $S(q) = (1/N)\langle\rho_{\boldsymbol{q}}\rho_{-\boldsymbol{q}}\rangle$ is the equilibrium static structure factor. For the force–force autocorrelation function, we obtain

$$\begin{aligned}\langle\boldsymbol{F}(0)\cdot\boldsymbol{F}(t)\rangle &= \langle\boldsymbol{F}(0)\cdot{\rm e}^{\Omega t}\cdot\boldsymbol{F}(0)\rangle \\ &\approx \sum_{q,k}\frac{\langle\boldsymbol{F}\rho_q^{\rm S}\rho_{-q}\rangle\langle\rho_q\rho_{-q}^{\rm S}{\rm e}^{\Omega t}\rho_k^{\rm S}\rho_{-k}\rangle\langle\rho_k\rho_{-k}^{\rm S}\boldsymbol{F}\rangle}{N^2S(q)S(k)}.\end{aligned} \tag{A5}$$

The second step of the derivation is to factorize the multipoint dynamical correlations $\langle\rho_q\rho_{-q}^{\rm S}{\rm e}^{\Omega t}\rho_k^{\rm S}\rho_{-k}\rangle$ into products

of two-point correlations. Hence, the four-point correlation in Eq. (A5) gives

$$\langle \rho_q \rho^{\rm S}_{-q} \mathrm{e}^{\Omega t} \rho^{\rm S}_k \rho_{-k} \rangle = NS(q) \Gamma_{\rm S}(q,t) \Gamma_{\rm C}(q,t) \delta_{q,k}, \tag{A6}$$

where δ is Kronecker's delta function and the propagator $\Gamma_{\rm S}(q,t)$ ($\Gamma_{\rm C}(q,t)$) is the normalized single-particle (collective) dynamic structure factor. Noting that $\boldsymbol{F} = -\nabla V(\boldsymbol{r})$, we find

$$\langle \boldsymbol{F} \rho^{\rm S}_q \rho_{-q} \rangle = -k_{\rm B}T \langle \boldsymbol{\nabla} \rho^{\rm S}_q \rho_{-q} \rangle = -\mathrm{i}qk_{\rm B}T\rho C(q) S(q), \tag{A7}$$

where the first equation in Eq. (A7) follows from integration by parts and the second equality follows from the relation $\langle \rho^{\rm S}_q \rho_{-q} \rangle = \rho C(q) S(q)$.[39] Combining all items and turning the sum into an integral, we obtain the memory function

$$\begin{aligned} K(t) &= \frac{\beta}{2} \langle \boldsymbol{F}(t) \cdot \boldsymbol{F}(0) \rangle \\ &= \frac{1}{2} k_{\rm B}T \int \frac{\mathrm{d}\boldsymbol{q}}{(2\pi)^2} q^2 C^2(q) \rho S(q) \Gamma_{\rm S}(q,t) \Gamma_{\rm C}(q,t). \end{aligned} \tag{A8}$$

In the third step of the procedure, we adopt a harmonic model of the amorphous solid state and Vineyard approximation. Then, the propagators yield

$$\Gamma_{\rm S}(q, t \to \infty) = \mathrm{e}^{-q^2/4\alpha}, \tag{A9}$$

$$\Gamma_{\rm S}(q, t \to \infty) = \mathrm{e}^{-q^2/4\alpha S(q)}, \tag{A10}$$

where the localization length $r^2_{\rm LOC} = 1/\alpha$. Finally, we obtain a self-consistent equation for $r^2_{\rm LOC}$ by taking the equipartition relation $\frac{1}{2} K_\infty r^2_{\rm LOC} = k_{\rm B}T$,

$$\begin{aligned} \frac{1}{r^2_{\rm LOC}} =& \frac{1}{4} \int \frac{\mathrm{d}\boldsymbol{q}}{(2\pi)^2} q^2 C^2(q) \rho S(q) \\ & \times \exp\left\{ -\frac{q^2 r^2_{\rm LOC}}{4} \left[1 + S^{-1}(q) \right] \right\}. \end{aligned} \tag{A11}$$

This suggests that the self-consistent equation can be restored by minimizing the dynamic free energy, i.e., $\partial F_{\rm eff}/\partial r = 0$. Hence, we can construct an expression for $F_{\rm eff}$ in Eq. (2).

In Eqs. (4) and (5), expressions for the elastic shear modulus and viscosity are derived to evaluate the stress–stress autocorrelation function $\langle \tau_i(t) \cdot \tau_j(0) \rangle$. Following the same line as above, we project the stress τ_i onto bilinear products of the collective density fluctuation, $\rho_q \rho_{-q}$, to obtain Eqs. (4) and (5).

In the normal liquid regime, independent binary collisions control the decay of the collective propagator. Under the de Gennes narrowing effect, the propagator and diffusion constant yield

$$\Gamma_{\rm C}(q,t) = \exp\left(-q^2 D^{\rm C}_{\rm S} t \right), \tag{A12}$$

$$D^{\rm C}_{\rm S}(q) = \frac{k_{\rm B}T\, \mathrm{d}(q)}{S(q)\zeta_{\rm S}}, \tag{A13}$$

where $\zeta_{\rm s} = \zeta_0 g(\sigma)$ is the short-time friction coefficient in colloidal suspensions. When $\phi > \phi_{\rm c}$, activated hopping events dominate the transport behavior. Hence, the short-time friction $\zeta_{\rm S}$ is modified to $\zeta_{\rm S} + \zeta_{\rm hop}$ to include barrier hopping. Then, we immediately obtain Eq. (6).

References

[1] Faupel F, Frank W, Macht M P, Mehrer H, Naundorf V, Rätzke K, Schober H R, Sharma S K and Teichler H 2003 *Rev. Mod. Phys.* **75** 237

[2] Larson R G 1999 *The Structure and Rheology of Complex Fluids* (New York: Oxford University Press)

[3] Ashcroft N W and Mermin N D 2005 *Solid State Physics* (New York: Holt, Rinehart and Winston)

[4] Berthier L and Biroli G 2011 *Rev. Mod. Phys.* **83** 587

[5] Saltzman E J and Schweizer K S 2003 *J. Chem. Phys.* **119** 1197

[6] Dyre J C 1987 *Phys. Rev. Lett.* **58** 792

[7] Arkhipov V and Bässler H 1995 *Phys. Rev. E* **52** 1227

[8] Bouchaud J P, Cugliandolo L, Kurchan J and Mézard M 1996 *Physica A* **226** 243

[9] Monthus C and Bouchaud J P 1996 *J. Phys. A: Math. Gen.* **29** 3847

[10] Berthier L 2003 *J. Phys: Condens. Matter* **15** S933

[11] Fuchs M and Cates M E 2002 *Phys. Rev. Lett.* **89** 248304

[12] Cates M E, Fuchs M, Kroy K, Poon W C and Puertas A M 2004 *J. Phys: Condens. Matter* **16** S4861

[13] Konig H, Hund R, Zahn K and Maret G 2005 *Eur. Phys. J. E* **18** 287

[14] Ebert F, Keim P and Maret G 2008 *Eur. Phys. J. E* **26** 161

[15] Mazoyer S, Ebert F, Maret G and Keim P 2009 *Europhysics. Lett.* **88** 66004

[16] Klix C L, Ebert F, Weysser F, Fuchs M, Maret G and Keim P 2012 *Phys. Rev. Lett.* **109** 178301

[17] Bayer M, Brader J M, Ebert F, Fuchs M, Lange E, Maret G, Schilling R, Sperl M and Wittmer J P 2007 *Phys. Rev. E* **76** 011508

[18] Henrich O, Weysser F, Cates M E and Fuchs M 2009 *Philos. Mag. R. Soc. London* **367** 5033

[19] Seyboldt R, Hajnal D, Weysser F and Fuchs M 2012 *Soft Matter* **8** 4132

[20] Schweizer K S and Saltzman E J 2003 *J. Chem. Phys.* **119** 1181

[21] Schweizer K S 2005 *J. Chem. Phys.* **123** 244501

[22] Mirigian S and Schweizer K S 2013 *J. Phys. Chem. Lett.* **4** 3648

[23] Mirigian S and Schweizer K S 2014 *J. Chem. Phys.* **140** 194506

[24] Mirigian S and Schweizer K S 2014 *J. Chem. Phys.* **140** 194507

[25] Dell Z E and Schweizer K S 2015 *Phys. Rev. Lett.* **115** 205702

[26] Chen K and Schweizer K S 2007 *Europhys. Lett.* **79** 26006

[27] Chen K and Schweizer K S 2009 *Phys. Rev. Lett.* **102** 038301

[28] Kobelev V and Schweizer K S 2005 *J. Chem. Phys.* **123** 164902

[29] Kobelev V and Schweizer K S 2007 *Phys. Rev. E* **71** 021401

[30] Zhang B K, Li H S, Tian W D, Chen K and Ma Y Q 2014 *J. Chem. Phys.* **140** 094506

[31] Zwanzig R 2001 *Nonequilibrium Statistical Mechanics* (New York: Oxford University Press)

[32] Verberg R, Schepper D I and Cohen E 1997 *Phys. Rev. E* **55** 3143

[33] Cohen E, Verberg R and Schepper D I 1998 *Physica A* **251** 251

[34] Hansen J P and McDonald I R 1990 *Theory of Simple Liquids* (Amsterdam: Elsevier)

[35] Wu J and Li Z 2007 *Annu. Rev. Phys. Chem.* **58** 85

[36] Guo X and Riebel U 2006 *J. Chem. Phys.* **125** 144504

[37] Hänggi P, Talkner P and Borkovec M 1990 *Rev. Mod. Phys.* **62** 251

[38] Eyring H 1936 *J. Chem. Phys.* **4** 283

[39] Gotze W 2008 *Complex Dynamics of Glass-forming Liquids* (New York: Oxford University Press)